

Pressure- and Temperature-Induced Phase Transitions in 2,4,6-Trichloro-1,3,5-triazine Crystal

Makiko Tanaka, Chinatu Kariu, Yoshio Suzuki,† Yoshinori Nibu, Ryoichi Shimada,† and Hiroko Shimada*

Department of Chemistry, Faculty of Science, Fukuoka University, Nanakuma, Jonan-ku, Fukuoka 814-0180

†Department of Electronics, Faculty of Technology, Fukuoka Institute of Technology, Wajiro-Higashi, Higashi-ku, Fukuoka 811-0295

(Received November 20, 2000)

The effects of pressure and temperature on the frequencies and band structures of the Raman active inter- and intramolecular vibrations of 2,4,6-trichloro-1,3,5-triazine crystal were studied. The changes in the Raman frequency, band width, and band structure of both the inter- and intramolecular vibrations induced by changes of pressure and temperature indicate that (1) a displacive phase transition caused by a shear distortion of π-stacked layer structure may take place under about 1.7 GPa at 298 K and (2) the intermolecular nitrogen–chlorine donor–acceptor attractive interactions supporting the extensive network structure in crystal have a direct effect upon the totally symmetric C–Cl stretching vibration.

The short nitrogen–halogen intermolecular contacts are a relatively common feature in crystalline organic solids of the halogen substituted heterocyclic compounds. The intermolecular nitrogen–halogen donor–acceptor interactions are weakly attractive, and play an important part in determining the structures of organic crystals.[1–3] 2,4,6-Trichloro-1,3,5-triazine (cyanuric chloride) crystallizes as notably slippery plates having a π-stacked layered structure, although other compounds having D_{3h} symmetry, such as 1,3,5-trihalobenzenes, pack in herringbone patterns in crystal. The cyanuric chloride crystal is made from extensive networks of intermolecular nitrogen–chlorine interactions.

The inter- and intramolecular vibrations of cyanuric chloride were studied experimentally[1–3] and theoretically.[4,5] The crystal structure was determined with X-ray analysis by Hoppe et al.[6] and reexamined by Pascal et al.[7,8]

We studied the phase transitions and intermolecular interactions in molecular crystals based on experimental and theoretical investigations of the temperature and pressure effects on the Raman active inter- and intramolecular vibrations of various molecular crystals, such as benzene,[9] halo-substituted benzenes,[10,11,12] methyl-substituted benzenes,[13] pyrazine,[14] and halo-substituted *p*-benzoquinone.[15] We pointed out in these works that the half-band widths plotted against pressure (pressure–band width curve) gave effective information for studying phase transitions in molecular crystals where spectral structure and vibrational frequencies plotted against pressure (pressure–frequency curve) did not clearly show discontinuous changes.[12,14,15]

This work is intended to study the intermolecular nitrogen–halogen donor–acceptor interactions in cyanuric chloride crystal through observations of pressure and temperature effects on the inter- and intramolecular vibrations, and also through a comparison with the results obtained for the pressure effects on the intramolecular vibrations of 1,3,5-trichlorobenzene crystal.

Experimental

Materials. Cyanuric chloride obtained from Kanto Chemicals was purified by zone-refining of about 100 passages. The sample was powdered as finely as possible with a mortar and pestle.

Optical Measurement. The Raman spectra of cyanuric chloride crystal due to the inter- and intramolecular vibrations were measured with a JOBIN-YVON T64000 laser Raman spectrophotometer under various pressures from 1 atm (1×10^{-4} GPa) to 4.5 GPa at 298 K and also at various temperatures from 298 to 77 K under ambient pressure by the backscattering observation method. The 488.0 and 476.5 nm beams from an Ar^+ ion laser of Spectra Physics were used for the excitation. A diamond anvil cell obtained from Toshiba Tungaloy Co. was used for measurements of the Raman spectra under various pressures. A cryostat of OXFORD DN1704 was used for measurements of the Raman spectra at various temperatures. The method of observing of the Raman spectra was essentially the same as that described previously.[10,11] A hole having a diameter of 0.3 mm was made in the center of a stainless-steel gasket whose thickness was 0.5 mm. The pressure inside the gasket hole was determined by measuring the wavelength shift of the R_1 fluorescence line at 694.2 nm emitted from the ruby chips according to the equation proposed by Mao et al.[16] The pressure inside the hole was confirmed to be hydrostatic by observing the shapes of the R_1 and R_2 (692.7 nm) fluorescence lines emitted from ruby.

Results and Discussion

Temperature Effects on the Intermolecular Vibrations. The crystal structure of cyanuric chloride belongs to monoclin-

Table 1. Raman Frequencies of the Intermolecular Vibrations of Cyanuric Chloride Crystal

Band	This work				Thomas et al.[a]		
	298 K (at 1 atm)	77 K (at 1 atm)	2 GPa (at 298 K)	4.5 GPa (at 298 K)	298 K (at 1 atm)	77 K (at 1 atm)	
	$\tilde{\nu}$/cm^{-1}	$\tilde{\nu}$/cm^{-1}	$\tilde{\nu}$/cm^{-1}	$\tilde{\nu}$/cm^{-1}	$\tilde{\nu}$/cm^{-1}	$\tilde{\nu}$/cm^{-1}	Assignment[b]
a	23	27					
b	31	35			33		R_z
c	64	72	85	100	66	71	R_x, R_y
d	74	83	113	143	77	84	R_x, R_y
e	93	103			97	104	T ?

a) Taken from Ref. 2. b) R_x, R_y, and R_z refer to the rotational intermolecular vibrations about x, y, and z axes, respectively. T refers to the translational intermolecular vibration.

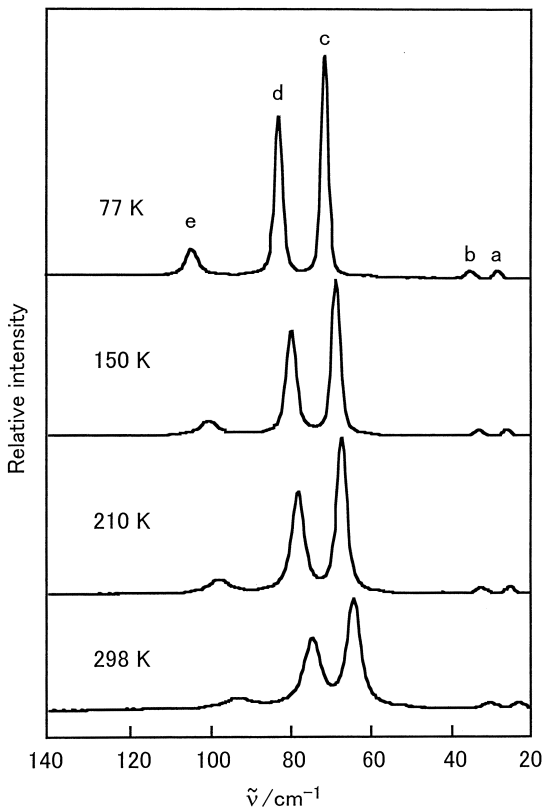

Fig. 1. The Raman spectra of cyanuric chloride crystal in the intermolecular vibrational region observed at various temperatures between 77 and 298 K under 1 atm.

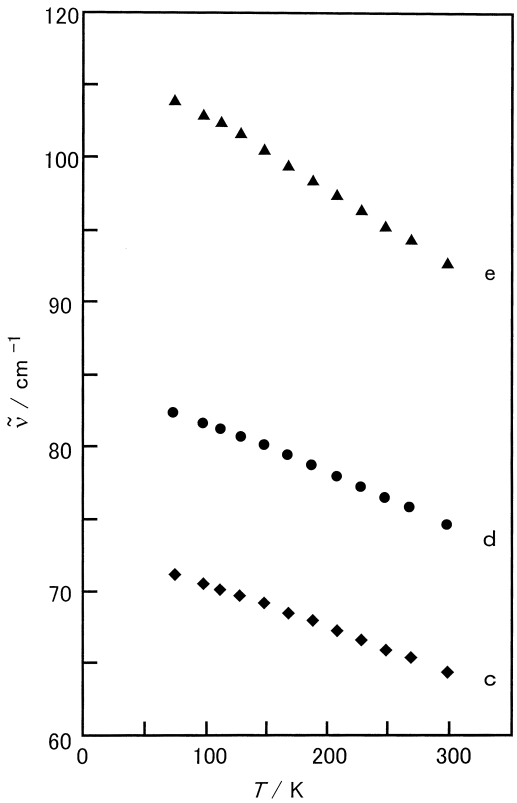

Fig. 2. Temperature–frequency curves for the Raman bands of cyanuric chloride crystal in the intermolecular vibrational region observed at various temperatures between 77 and 298 K under 1 atm.

ic space group $C2/c$ at 300 K with four molecules in a unit cell. The symmetry of the molecular geometry of cyanuric chloride is closely approximated by the D_{3h} point group.[8] The Raman spectra measured at various temperatures under 1 atm are shown in Fig. 1, and the vibrational frequencies of the observed bands are given in Table 1. Thomas et al.[2] discussed the intermolecular vibrations of cyanuric chloride crystal and gave an assignment for the observed bands b, c, d, and e shown in Fig. 1. The vibrational frequencies and half-band widths plotted against temperatures are shown in Figs. 2 and 3, respectively. The vibrational frequencies and half-band widths were obtained by a curve-fitting method using the Voight function in order to determine the reasonable frequencies and band widths of the band peaks. These curves are referred to as temperature–frequency and temperature–band width curves, respectively. Figures 1, 2, and 3 show that (1) the spectral structure composed of five bands (a, b, c, d, e) remains unchanged with decreasing temperature, (2) the slopes of the temperature–frequency curves increase monotonously and continuously with decreasing temperature, and (3) the slope of the temperature–band width curve for band e shows a slightly discontinuous behavior at about 150 K. These observed facts indicate that no drastic phase transition accompanied by a change in the symmetry of crystal structure takes place in cyanuric chloride crystal in the temperature range from 298 to 77 K, though the relaxation processes resulting from intermolecular interactions may change slightly at about 150 K. The thermograms obtained with a differential scanning calorimetry for the crystal

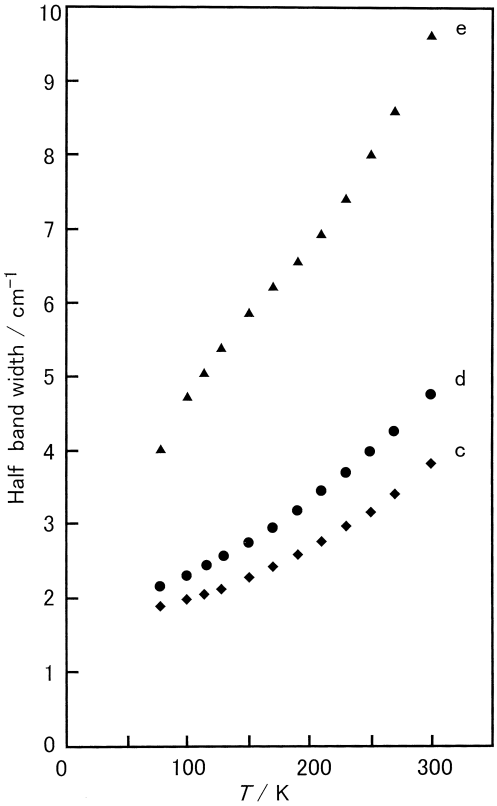

Fig. 3. Temperature-band width curves for the Raman bands of cyanuric chloride crystal in the intermolecular vibrational region observed at various temperatures between 77 and 298 K under 1 atm.

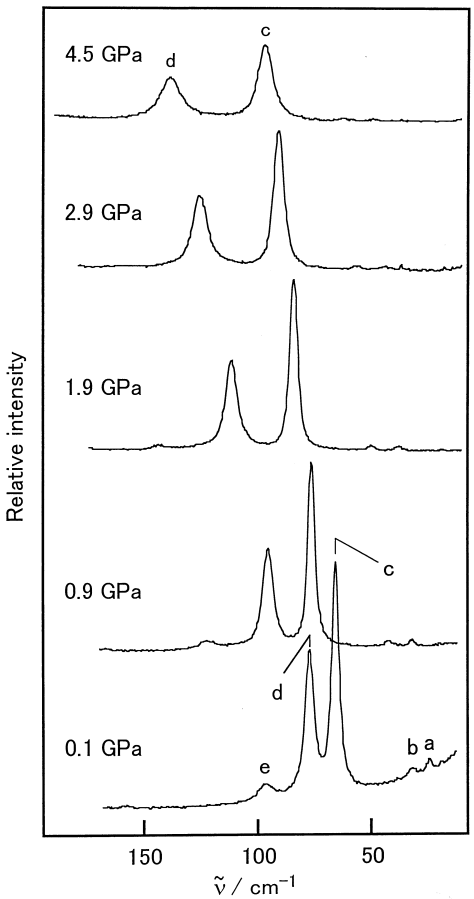

Fig. 4. The Raman spectra of cyanuric chloride crystal in the intermolecular vibrational region observed under various pressures between 0.1 and 4.5 GPa at 298 K.

show no endothermic peaks at between 77 and 298 K

Pressure Effects on the Intermolecular Vibrations. The Raman spectra of cyanuric chloride crystal observed in the intermolecular vibrational region under various pressures at 298 K are shown in Fig. 4, and the vibrational frequencies are given in Table 1. The spectrum observed under 0.1 GPa mainly consists of five bands (a, b, c, d, e) and the spectral structure is essentially the same as that shown in Fig. 1, except for the fact that the weak bands (a, b, e) could not be clearly resolved under higher pressure. The spectral structure does not change with successive applications of pressure. The vibrational frequencies and half-band widths plotted against pressure for bands c and d are shown in Figs. 5 and 6, respectively. These curves will be referred to as pressure–frequency and pressure–band width curves, respectively. These figures show that the slopes of the pressure–frequency curves increase monotonously and continuously with increasing pressure, though the slopes of the pressure–band width curves show clearly discontinuous behavior under about 1.7 GPa. These observed facts indicate that no drastic phase transition takes place in cyanuric chloride crystal in the pressure range from 1 atm to 4.5 GPa, but that the relaxation processes resulting from the intermolecular interactions change under about 1.7 GPa, suggesting a displacive phase transition under about 1.7 GPa.

Pressure Effect on Intramolecular Vibrations of Cyanuric Chloride. The Raman spectra observed under various pressures at 298 K are shown in Fig. 7. The Raman bands observed at 175, 216, 408, 474, and 977 cm^{-1} under 1 atm were assigned to the intramolecular vibrations of ν_{10} (Cl wagging of e″ symmetry species), ν_{18} (Cl bending of e′ species), ν_{13} (C–Cl stretching of a_1' species), ν_{20} (C–Cl stretching of e′ species), and ν_1 (ring breathing of a_1' species), respectively,[2,3] where the nomenclature of the vibrational modes are taken from that given by Mair and Honig.[17] These five bands are clearly observed under high pressures up to 4.5 GPa and their vibrational frequencies are given in Table 2. The observed frequency shifts, defined by $\Delta\tilde{\nu} = \tilde{\nu}_{p\ \mathrm{GPa}} - \tilde{\nu}_{1\ \mathrm{atm}}$, are plotted against pressures, and the curves are shown in Fig. 8. The observed curve for the ν_{13} mode of 1,3,5-trichlorobenzene is also shown in Fig. 8 in order to compare the curve of the ν_{13} mode of cyanuric chloride.

It was shown in previous work[9–15] that the slope of the pressure–frequency shift curve becomes continuously smaller with increasing pressure, and that the curve bends slightly downward when a phase transition does not take place upon applying pressure. Figure 8 shows the following facts: (1) The slopes of the pressure–frequency shift curves for the ν_{18}, ν_1, and ν_{20} vibrational bands become continuously smaller with increasing pressure up to 4.5 GPa and the curves bend slightly downward. (2) The pressure-induced frequency shift for the ν_{10} band is larger than the shifts for the ν_{18}, ν_1, and ν_{20} bands

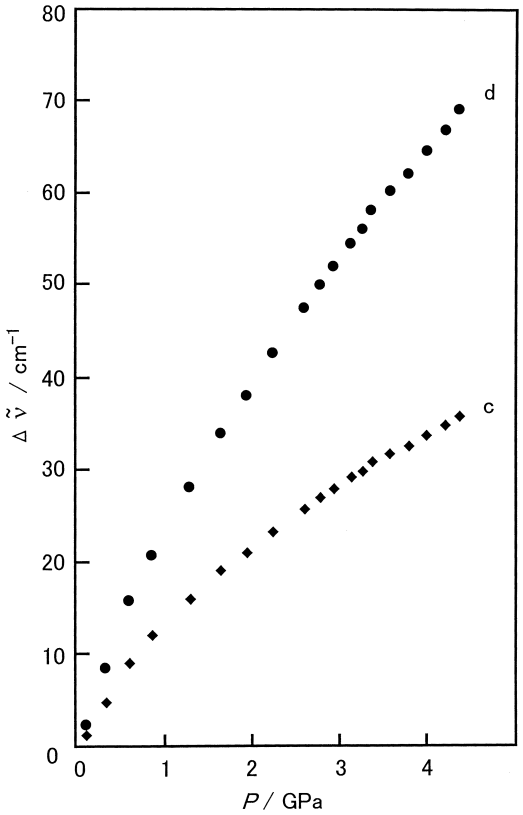

Fig. 5. Pressure–frequency curves for the Raman bands of cyanuric chloride crystal in the intermolecular vibrational region observed under various pressures between 1 atm and 4.5 GPa at 298 K.

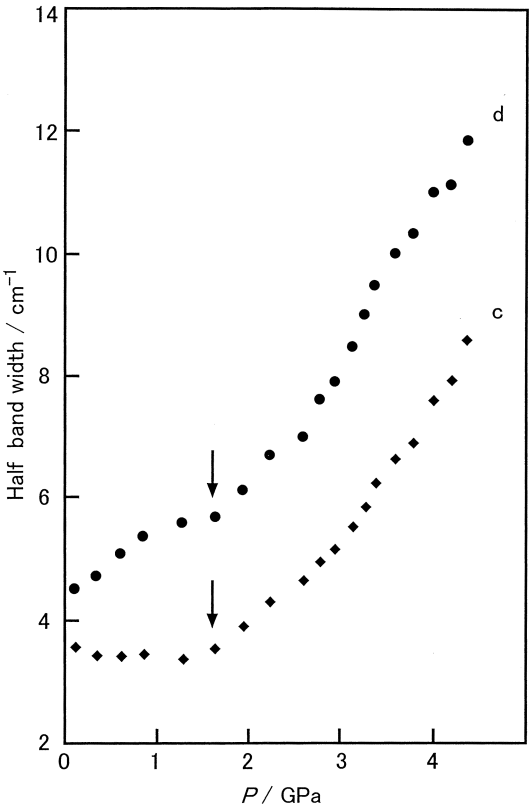

Fig. 6. Temperature-band width curves for the Raman bands of cyanuric chloride crystal in the intermolecular vibrational region observed under various pressures between 1 atm and 4.5 GPa at 298 K.

and the pressure–frequency shift curve bends slightly upward. (3) The behavior of the pressure-induced frequency shift for the ν_{13} band of cyanuric chloride is different from the behavior of the ν_{18}, ν_1, and ν_{20} bands, and the shift becomes almost constant above 2.8 GPa. (4) The pressure-induced frequency shift for the ν_{13} band of 1,3,5-trichlorobenzene increases gradually with increasing pressure up to 4.5 GPa, as in the ν_{18}, ν_1, and ν_{20} bands of cyanuric chloride.

The pressure-induced frequency shifts of the intramolecular vibrations caused by the intermolecular interactions of neighboring eight molecules were calculated for the ν_{10}, ν_{18}, ν_{13}, ν_{20}, and ν_1 vibrations under various pressures from 1 atm to 4.5 GPa in the same way as described previously.[9–15] The frequency shift of the intramolecular vibrations induced by the intermolecular interaction with other molecules are calculated by[9–15]

Table 2. Frequencies of the Raman Active Intramolecular Vibrations of Cyanuric Chloride Crystal

Sym	Band	This work				Thomas[a)]	Navarro[b)]
		298 K (at 1 atm)	77 K (at 1 atm)	2 GPa (at 298 K)	4.5 GPa (at 298 K)	298 K (at 1 atm)	
		$\tilde{\nu}$/cm^{-1}	$\tilde{\nu}$/cm^{-1}	$\tilde{\nu}$/cm^{-1}	$\tilde{\nu}$/cm^{-1}	$\tilde{\nu}$/cm^{-1}	$\tilde{\nu}$/cm^{-1}
	ν_{12} (Ring)					1297	1293
a_1'	ν_1 (Ring)	977	980	986	996	977	981
	ν_{13} (C–Cl str)	408	408	416	418	408	404
	ν_8 (Ring)	1498	1501			1520	1500
	ν_{19} (Ring)	1257	1261			1260	1264
e'	ν_6 (Ring)	847				849	847
	ν_{20} (C–Cl str)	474	475	485	496	474	466
	ν_{18} (Cl bend)	216	219	223	230	216	221
e''	ν_{16} (Ring)	651	652			652	647
	ν_{10} (Cl wag)	175	182	182	202	178	186

a) Taken from Ref. 2. b) Taken from Ref. 3.

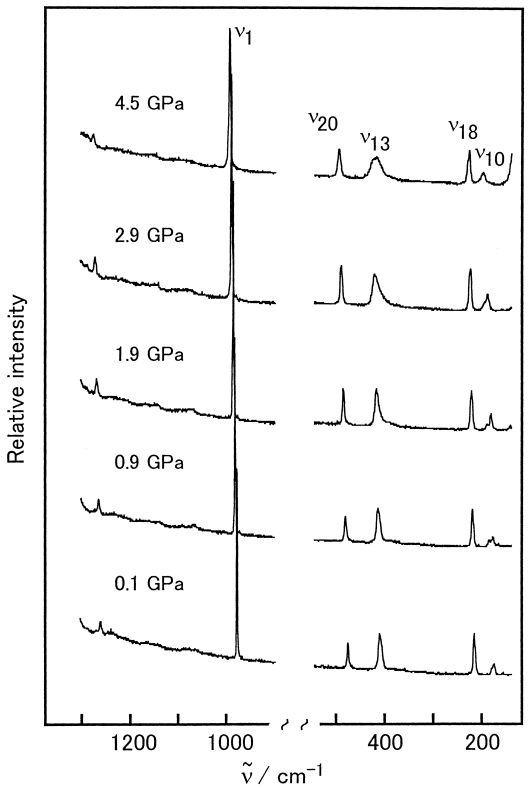

Fig. 7. The Raman spectra of cyanuric chloride crystal in the intramolecular vibrational region observed under various pressures between 0.1 and 4.5 GPa at 298 K.

$$\Delta\tilde{\nu}_{\text{shift}} = \frac{1}{8\pi^2 c^2 \tilde{\nu}_{Qn}} \sum_i \sum_j \left(\frac{\partial^2 V_{ij}}{\partial r_{ij}^{\,2}}\right)\left(\frac{\partial r_{ij}}{\partial Q_n}\right)^2,$$

where Q_n and $\tilde{\nu}_{Qn}$ are the n-th normal coordinate and its unperturbed vibrational frequency, respectively, r_{ij} is the interatomic distance between atoms i and j belonging to different molecules, and V_{ij} is the potential energy of the atom–atom type due to the intermolecular interaction between two molecules. For the potential V_{ij},

$$2\,V_{ij} = [-Ar_{ij}^{-6} + B\exp(-Cr_{ij})] \quad (1)$$

was used, where A, B, and C are parameters. The values of the parameters were taken from those given by Spackman.[18] The first and second terms in Eq. 1 represent the dispersive and repulsive energies, respectively. The values of the compressibility of the cyanuric chloride crystal were not reported and, thus, the values were approximated by the values given for the hexachlorobenzene crystal.[11]

The displacement vectors of the atoms due to the normal vibrations of the cyanuric chloride molecule, which are necessary to calculate the pressure-induced frequency shifts, were obtained from a normal coordinate calculation by the standard GF matrix method. The F-matrix elements for the in-plane and out-of-plane vibrations were evaluated with the potential of an improved modification of the Urey–Bradley and the valence force fields, respectively, in the same way as described previously.[19,20]

The values of the force constants for the in-plane and out-of-plane vibrations are given in Table 3. The notations of the force constants are the same as those described previously.[19,20] The values of the calculated frequency shifts induced by the repulsive and dispersion forces for the ν_{10a}, ν_{10b}, ν_{18a}, ν_{18b}, ν_{13}, ν_{20a}, ν_{20b}, and ν_1 vibrations under 1 atm and 4.5 GPa are given in Table 4. The calculated pressure–frequency shift curves are shown in Fig. 8, together with the observed curves, where the

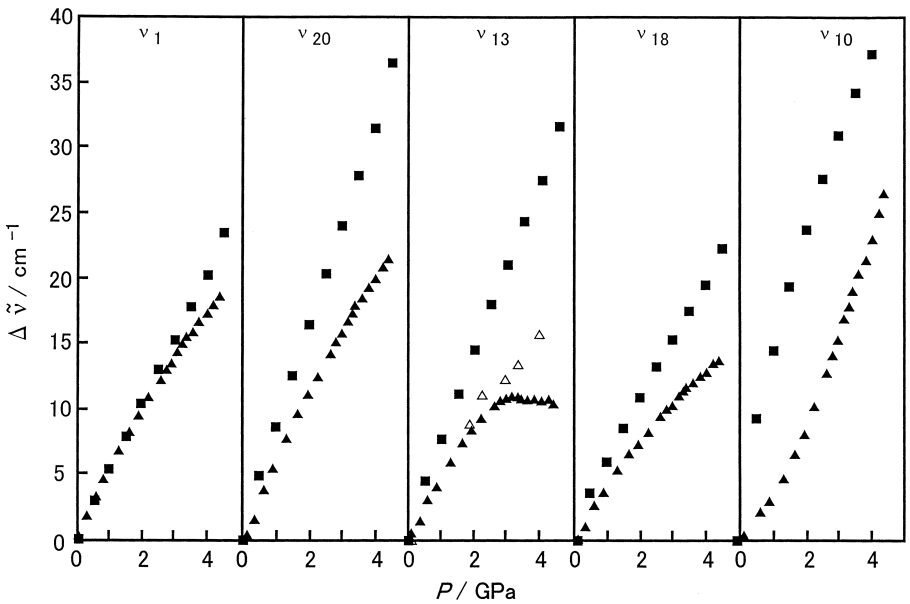

Fig. 8. Observed (▲) and calculated (■) pressure–frequency shift curves for the intramolecular ν_1, ν_{20}, ν_{13}, ν_{18}, and ν_{10} vibrations of cyanuric chloride cyrystal. The frequency shift $\Delta\tilde{\nu}$ is defined by ($\tilde{\nu}_{p\,\text{GPa}} - \tilde{\nu}_{1\,\text{atm}}$). Observed pressure–frequency shift curve for the ν_{13} vibration of 1,3,5-trichlorobenzene crystal is also shown by Δ.

Table 3. Force Constants for the Normal Vibrations of Cyanuric Chloride

In-plane vibration		Out-of-plane vibration	
$K_{N–C}$	4.9	$Q_{N–C}$	0.22
$K_{C–Cl}$	3.1	P_{Cl}	0.37
H_{NCN}	0.53	q^o	−0.02
H_{CNC}	0.55	q^m	0.02
H_{NCCl}	0.35	q^p	−0.02
$F_{N\cdots N}$	0.5	p^m	−0.05
$F_{C\cdots C}$	0.45	t^o	0.03
$F_{N\cdots Cl}$	0.7	t^m	−0.03
ρ	0.23		
$k^m_{r_{Cl}r_{Cl}}$	0.05		
$f^m_{\beta_{Cl},\beta_{Cl}}$	−0.05		

Force constants denoted by K, H, F, k, and ρ are given in hN m^{-1} (= mdyn/Å) units. f and Q, P, p, q, and t are in aNm rad^{-2} (= mdynÅ/rad^2) units. r_{Cl} and $_{\beta Cl}$ refer to the the C–Cl bond and the ∠NCCl, respectively. Superscripts o and m refer to ortho and meta, respectively.

curves are given only for a modes in the degenerated vibrations.

The calculation gives the following results. (1) The repulsive and dispersion forces contribute a large positive and a small negative values for the pressure-induced frequency shift, respectively, and therefore, the calculated frequency shift increases monotonously with increasing pressure for all vibrations. (2) The repulsive force between the chlorine and nitrogen atoms belonging to different molecules gives the largest contribution to the frequency shift for both the in-plane and out-of-plane vibrations. (3) The intermolecular interactions between molecules laying in the same layer work effectively for the frequency shift of the in-plane vibrations, while the intermolecular interactions between molecules laying in the upward and downward π-stacked layers work effectively for the frequency shift of the out-of-plane vibrations.

The agreement in the observed and calculated pressure-induced frequency shifts for the ν_1 mode is satisfactory well. However, the discrepancy of the observed and calculated frequency shifts becomes larger for the ν_{18} and ν_{20} modes from a pressure about 1.5 GPa, and the discrepancy is large even in the low pressure region for the ν_{10} mode. The observed pressure–frequency shift curve for the ν_{13} mode of cyanuric chloride deviates extremely from the calculated curve from a pressure above 2.8 GPa.

The attractive intermolecular interactions, such as the dispersion force, contribute negative values for the pressure-induced frequency shift. Therefore, the observed behavior of the ν_{13} mode suggests that a certain kind of attractive force acts on the molecules in the cyanuric chloride crystal in addition to the dispersion force. This additional attractive force may be attributed to the intermolecular nitrogen–chlorine donor–acceptor interactions supporting extensive networks in the cyanuric chloride crystal. The negative shift due to the intermolecular nitrogen–chlorine donor–acceptor interaction is small compared with the positive shift due to repulsive force under 1 atm. The application of pressure gives rise to a shortening of the intermolecular distance of the nitrogen and chlorine atoms, and a negative frequency shift due to the nitrogen–chlorine interactions becomes large. As a result, a negative frequency shift due to the nitrogen–chlorine interactions becomes to compete with the positive shift due to the repulsive interaction and, therefore, the observed shift becomes to be nearly constant above 2.8 GPa. The increment of the nitrogen–chlorine interactions in the same layer induced by the application of pressure stabilizes the extensive network structure of the cyanuric chloride crystal. The observed monotonous increase of the pressure-induced frequency shift for the ν_{13} mode of 1,3,5-trichlorobenzene by application of pressure is due to the fact that the attractive donor–acceptor interaction does not act on the molecules in the 1,3,5-trichlorobenzene crystal, where the molecules pack in herringbone patterns.

The reason why the intermolecular nitrogen–chlorine donor–acceptor interaction was not apparently detected for the C–Cl stretching ν_{20} mode of e′ symmetry species, but the interaction was clearly detected for the C–Cl stretching ν_{13} mode of a_1' symmetry species, can now be explained. The three out-of-phase C–Cl stretching displacements are characteristic of the ν_{20} mode, while the three in-phase displacements are characteristic of the ν_{13} mode. Therefore, the nitrogen–chlorine interactions can be detected prominently in the ν_{13} mode. The discrepancy in the observed and calculated frequency shifts above 1.5 GPa for the ν_{20} and ν_{18} modes is partially attributed to the donor–acceptor interactions.

Table 4. Calculated and Observed Pressure-induced Frequency Shifts of Some Raman Active Intramolecular Vibrations of Cyanuric Chloride Crystal

Mode	Calculated frequency shift						Frequency shift	
	$\tilde{\nu}_1$ atm			$\tilde{\nu}_{4.51}$ GPa			$\tilde{\nu}_{4.5}$ GPa − $\tilde{\nu}_1$ atm	
	Repul	Disp	Total	Repul	Disp	Total	Calcd	Obsd
	$\tilde{\nu}$/cm^{-1}	$\tilde{\nu}$/cm^{-1}	$\tilde{\nu}$/cm^{-1}	$\tilde{\nu}$/cm^{-1}	$\tilde{\nu}$/cm^{-1}	$\tilde{\nu}$/cm^{-1}	$\tilde{\nu}$/cm^{-1}	$\tilde{\nu}$/cm^{-1}
ν_{18a}	6.7	−1.8	4.9	32.0	−4.8	27.2	22.3	} 14
ν_{18b}	6.8	−1.8	5.0	38.8	−5.2	33.6	28.6	
ν_{13}	6.3	−1.3	5.0	41.4	−4.7	36.7	31.7	10
ν_{20a}	6.6	−1.4	5.2	46.9	−5.2	41.7	36.5	} 22
ν_{20b}	6.2	−1.3	4.9	43.6	−4.9	38.7	33.8	
ν_1	3.7	−0.7	3.0	29.5	−3.0	26.5	23.5	19
ν_{10a}	28.6	−6.6	22.0	75.5	−13.2	62.3	40.3	} 27
ν_{10b}	30.0	−6.9	23.1	77.8	−13.7	64.1	41.0	

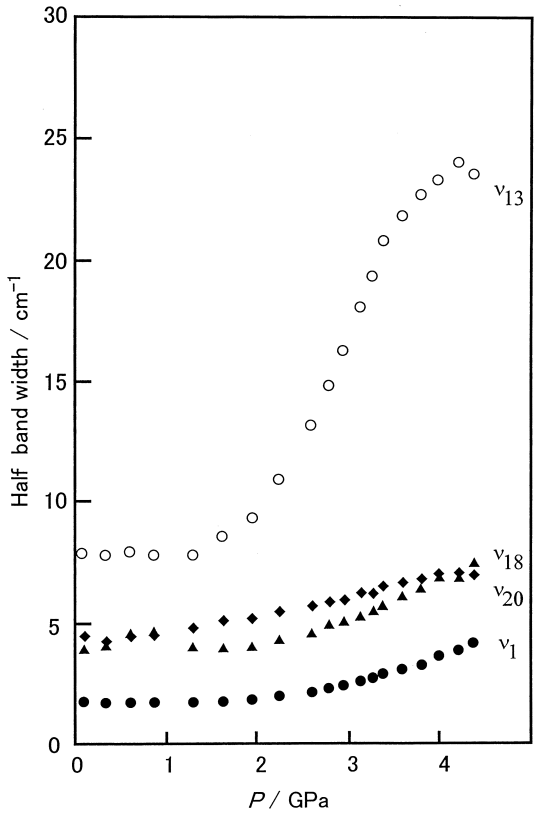

Fig. 9. Pressure-band width curves for the ν_{13} (○), ν_{18} (◆), ν_1 (●), and ν_{20} (▲) vibrations of cyanuric chloride crystal.

The fact that the slope of the pressure–frequency shift curve for the ν_{10} mode bends slightly upward suggests that the pressure–frequency shift curve for the ν_{10} mode should be decomposed into at least two components, that is, the intermolecular interactions change under a certain pressure between 1 atm and 4.5 GPa. It was analyzed that a discontinuous change in the slope of the pressure–frequency shift curve occurs under about 1.7 GPa for the ν_{10} mode. The observed frequency shift is especially larger for the ν_{10} mode involving the out-of-plane displacements of the Cl atoms than for the ν_{20} and ν_{18} modes involving the in-plane displacements of the Cl atoms. These prominent pressure effects on the out-of-plane ν_{10} mode may suggest that the π-stacked layer structure is strongly affected by applying pressure. It may be considered that a displacive phase transition takes place under 1.7 GPa in order to reduce large repulsive intermolecular interactions related to the Cl atoms and the displacive phase transition might be caused by a shear distortion of a π-stacked layer structure.

The half-band widths plotted against pressure (pressure–band width curve) are shown in Fig. 9. The slope of the pressure–band width curve for the ν_{13} mode clearly shows a discontinuous behavior under about 1.7 GPa. This fact also supports the fact that the intermolecular relaxation processes change and the displacive phase transition may take place under about 1.7 GPa. The half band widths for the weak ν_{10} band could not be resolved because of an overlapping of the other bands in the ν_{10} band region.

In conclusion, the intermolecular attractive nitrogen–chlorine donor–acceptor interactions give negative values for the pressure-induced frequency shift, which compensate for the large positive values due to the intermolecular repulsive interaction. The nitrogen–chlorine interactions act effectively on the extensive network structure in cyanuric chloride crystal. A displacive phase transition may be caused by a shear distortion of the π-stacked layer structure.

References

1 J. E. Lancaster and B. P. Stoicheff, *Can. J. Phys.*, **34**, 1016 (1956).
2 D. M. Thomas, J. B. Bates, A. Bandy, and E. R. Lippincott, *J. Chem. Phys.*, **53**, 3698 (1970).
3 A. Navarro, J. J. L. González, G. J. Kearley, J. Tomkinson, S. F. Parker, and D. S. Sivia, *Chem. Phys.*, **200**, 395 (1995).
4 A. Navarro, J. J. L. González, M. F. Gómez, F. Márquez, and J. C. Otero, *J. Mol. Struct.*, **376**, 353 (1996).
5 G. J. Kearley, J. Tomkinson, A. Navarro, J. J. L. González, and M. F. Gómez, *Chem. Phys.*, **216**, 323 (1997).
6 W. Hoppe, H. U. Lenne, and G. Morandi, *Z. Kristallogr.*, **108**, S. 321 (1957).
7 R. A. Pascal, Jr. and D. M. Ho, *Tetrahedron Lett.*, **33**, 4707 (1992).
8 K. Xu, D. M. Ho, and R. A. Pascal, Jr., *J. Am. Chem. Soc.*, **116**, 105 (1994).
9 H. Shimada, H. Kawano, Y. Suzuki, Y. Nibu, and R. Shimada, *Fukuoka Univ. Sci. Reports*, **25**, 109 (1995).
10 S. Matsukuma, H. Kawano, Y. Nibu, H. Shimada, and R. Shimada, *Bull. Chem. Soc. Jpn.*, **67**, 1588 (1994).
11 G. Sadakuni, M. Maehara, H. Kawano, Y. Nibu, H. Shimada, and R. Shimada, *Bull. Chem. Soc. Jpn.*, **67**, 1593 (1994).
12 H. Mizobe, H. Shimada, and R. Shimada, *J. Quan. Chem.*, **72**, 287 (1999).
13 F. Shimizu, K. Yoshikai, H. Kawano, Y. Nibu, H. Shimada, and R. Shimada, *Bull. Chem. Soc. Jpn.*, **69**, 947 (1996).
14 M. Maehara, H. Kawano, Y. Nibu, H. Shimada, and R. Shimada, *Bull. Chem. Soc. Jpn.*, **68**, 506 (1995).
15 A. Ikuta, K. Suzuki, Y. Nibu, H. Shimada, and R. Shimada, *Bull. Chem. Soc. Jpn.*, **72**, 963 (1999).
16 H. K. Mao, P. M. Bell, J. W. Shaner, and D. J. Steinberg, *J. Appl. Phys.*, **49**, 3276 (1978).
17 R. D. Mair and D. F. Hornig. *J. Chem. Phys.*, **17**, 1236 (1949).
18 M. A. Spackman, *J. Chem. Phys.*, **85**, 6579 (1986).
19 S. Kizuki, Y. Ishibashi, H. Shimada, and R. Shimada, *Mem. Fac. Sci. Kyushu Univ. Ser. C*, **13**, 7 (1981).
20 Y. Ishibashi, F. Arakawa, H. Shimada, and R. Shimada, *Bull. Chem. Soc. Jpn.*, **56**, 1327 (1983).